Effect of Riblets on the Streaky Structures Excited by Free Stream Tip Vortices in Boundary Layer

Andrey V. Boiko
Institute of Theoretical and Applied Mechanics,
Siberian Branch of the Russian Academy of Science,
Institutskaya Str., 4/1. 630090 Novosibirsk, Russia
Kwang Hyo Jung, Ho Hwan Chun, Inwon Lee*
Advanced Ship Engineering Research Center, Pusan National University,
Busan 609-735, Korea

In this study, experimental investigations were made regarding the effect of riblets on the streak instability in boundary layer. The streak instability is now regarded as a major source of the self-regeneration mechanism for the hairpin type coherent structures in turbulent boundary layer flow. Thus, it is important to control the instability to suppress the drag-inducing vortical structure in terms of drag reduction. Toward enhancing the measurement accuracy and spatial resolution, an enlarged version of riblets was applied to a streak which was artificially induced by a microwing in a laminar boundary layer. It is found that the riblets have attenuation effect on the streak instability, i.e., to reduce the spanwise velocity gradient of the quasi-streamwise streak in boundary layer.

Key Words : Boundary Layer Control, Streaky Structure, Riblet

Nomenclature

U_0 : Freestream velocity
u' : Turbulence intensity
x_0 : Location of the microwing/roughness elements in the streamwise coordinate
y_0 : Location of the microwing/roughness elements in the wall-normal coordinate
δ^* : Displacement thickness of the boundary layer

1. Introduction

The significant role of streamwise vortices in laminar-turbulent transition and viscous sublayer of turbulent boundary layer suggests the possibility of their control. Kline et al.(1967) were the first who marked a similarity between transitional structures and coherent motion in the near-wall viscous region of a turbulent boundary layer. Discussions on this analogy and additional references are contained, e.g. in papers by Blackwelder (1983) and Kachanov (1994). It is believed that the mechanisms of formation and breakdown of the structures are the same in both cases. The external vortical disturbances in the form of localized quasi-stationary flow modulations or free-stream turbulence are of those which most frequently contribute to the boundary-layer disturbances. From this point of view, two types of phenomena are usually distinguished inside the boundary layer : the generation of travelling modes with characteristics of local linear instability and the generation of quasi-stationary longitudinal (vortical) structures or 'streaks', of which characteristics seems are usually determined by the external vortical disturbances. These phenomena are considered to be responsible for the transition to turbulence. The experimentally observed disturbance motion produced by the streaks is sometimes re-

* Corresponding Author,
E-mail : inwon@pusan.ac.kr
TEL : +82-51-510-2764; **FAX** : +82-51-581-3718
Advanced Ship Engineering Research Center, Pusan National University, Busan 609-735, Korea. (Manuscript **Received** July 7, 2006; **Revised** October 20, 2006)

ferred to as a 'Klebanoff mode', due to early observations of Klebanoff et al.(1962), who found steady and low-frequency spanwise periodic modulations of the streamwise velocity component in the Blasius boundary layer produced by a residual inhomogeneity raised by wind tunnel damping screens. Later the mean and fluctuating characteristics of the flat plate boundary layer subject to the 3D free-stream disturbances in the form of nearly isotropic freestream turbulence has been studied extensively, e.g., in Westin et al.(1994) and Boiko et al.(1994), and led to a selection of a series of phenomenological characteristics inherent for the 'streak' motion inside boundary layers.

A number of techniques have been proposed for turbulence control in the viscous sublayer to reduce skin-friction drag. A recent review has been compiled by Gad-el-Hak (1990). It is known that some of these control techniques, for example, surface modifications, also affect disturbance development in transitional flows. Advanced methods to reduce the turbulent skin-friction drag include surface modifications in the form of riblets, i.e., streamwise micro-grooves of various shapes located on the surface. Historically, the idea to use the riblets arose in the middle of the 1960's (Berchert and Bartenwerfer 1989) through an analysis of the skin of high-speed sharks. Some types of riblets, interacting favorably with near-wall flow, produce skin-friction drag reduction in spite of the increase of the surface area. A net drag reduction of about 6% is achieved with V-shape riblets, the riblets being effective in the presence of moderate pressure gradients. It has become evident that the riblets introduce an anisotropy in the near-wall motions, but definite conclusions on the physics of their influence on turbulent drag arc far from being drawn, although recently some progress in understanding the mechanisms of the phenomenon has been achieved. Pioneering studies by Walsh (1983) and later experiments have shown that the optimum heights and spacings of the symmetric triangular riblets are about 15-20 wall units. Bechert and Bartenwerfer (1989) and Choi (1989) pointed out independently that the optimal riblet spacing is close to the characteristic size of the near-wall coherent streaks. It has also been proved that the riblets significantly modify the streak activity and proposed that among other possible mechanisms, a restriction of spanwise momentum of the streamwise vortices close to the wall by the riblets with sharp tips would have a prime responsibility for the drag reduction. Direct numerical simulations by Choi et al.(1993), and theoretical results by Luchini et al.(1991) are in accordance with this idea. By means of experimental simulations, Grek et al.(1993) could separate the riblet effect on different stages of the transition on a flat plate. They showed that the riblets placed in the region of linear development of a Tollmien-Schlichting wave can destabilize its growth and encourage transition, while, on the contrary, the same riblets placed in the region of formation and development of a nonlinear three-dimensional flow or beneath stationary streamwise vortices delays flow breakdown into turbulence. These experiments are able to resolve the uncertainty of previous studies; they show that the riblets can significantly inhibit the later stages of transition to turbulence, while accelerating the earlier ones. Later Grek et al.(1995) considered a model of the combined effect of riblets on the development of streamwise velocity modulations and travelling waves. The experiments showed that the effect of the riblets is to suppress the activity of an array of symmetric streamwise vortices excited in a flat plate boundary layer. At the same time, the boundary layer becomes stable with respect to high-frequency traveling waves which cause transition in the absence of the riblets. In previous studies offering explanations of the riblets effect upon near-wall structures e.g., Choi (1991), Grek et al.(1995), the presence of counter-rotating vortex pairs is supposed. At the same time, there are few experiments on riblet-control in transitional as well as turbulent asymmetric flows (e.g., Coustols 1992; Schneider and Dinkelacker 1992).

The experiments described below were carried out with the intention to look at the riblets effect on transition in an isolated vortex of large magnitude, excited in a boundary-layer by a vortex generator where a swept wing with a secondary mean flow at its leading edge serves as a tool for

such vortex generation. In the present study free stream axial vortex of controlled strength and position was used to generate an isolated streak in Blasius boundary layer. It has already been proved that the streak models significant features of effect of free stream turbulence onto the boundary layer in natural conditions (Boiko 2002). The streak grew downstream essentially linearly with the streamwise coordinate. It was shown that the disturbance characteristics are in agreement with data of previous experiments performed under natural and control conditions concerning the 'by-pass' transition initiated at high free stream disturbance levels.

2. Experimental Appratus

2.1 Wind tunnel and test section

The experiments were performed on a 695×1,200 mm^2 flat plate model mounted in the wind tunnel at the Aerospace Department of Pusan National University. This tunnel has a 2 m long test section with a cross section of 0.7×0.7 m^2. Wind tunnel specifications are shown in Fig. 1. Mean and fluctuating streamwise velocity components were obtained with miniature constant-temperature Dantec Dynamics hot-wire anemometers using I-arranged hot wire probe. The MiniCTA system is a versatile anemometer that is widely used in air flows for accurate measurements. It is especially suitable for basic flow diagnostics and its small size facilitates mounting close to the probe or even for it to be built into flow models. It contains also an analog signal conditioner consisted of differential amplifiers with voltage offset used to subtract fixed constant voltages from the bridge and to improve the system dynamic range and resolution of sampled signal. Signals from the hot-wire anemometer bridge was digitized by National Instruments 12-digit A/D converter PCI-6023E. The length of records was two seconds with sampling frequency 350 Hz. The samples were processed with a personal computer in MATLAB environment.

The wire was calibrated against a Pitot-Prandtl tube in free stream. The free stream velocity was recovered by using Pitot-Prandtl tube placed close to the hot-wire. The flat plate model was 1,565 mm long, 695 mm wide, and 10 mm thick. The model consists of a main Plexiglas body, a trailing edge flap and a leading edge. The leading edge is elliptical with the axis-ratio 6 : 1 to eliminate possible leading edge separation. The flap was used to obtain a smooth pressure distribution without the so-called suction peak at the leading edge (see Fig. 2).

The model was vertically installed along the test section axis, as shown in Fig. 3. The large

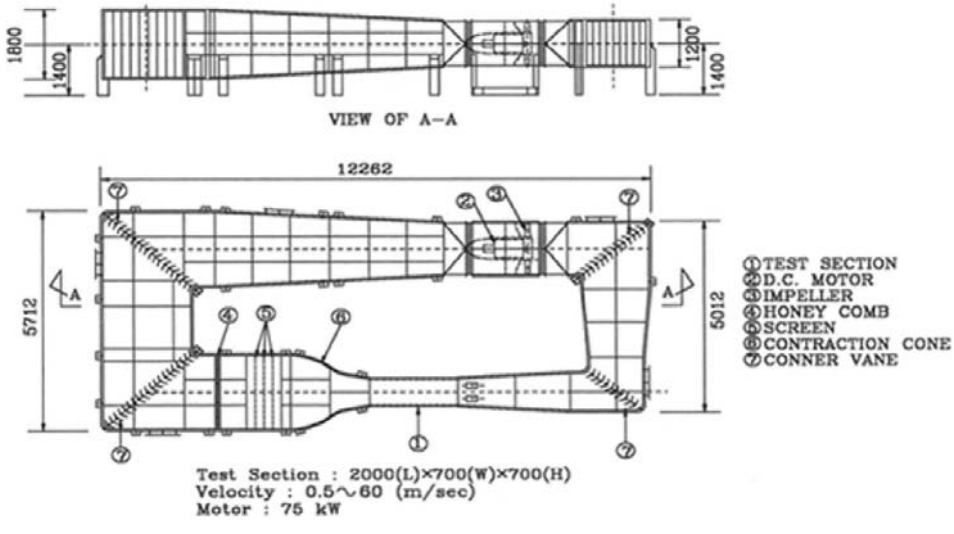

Fig. 1 Schematic diagram of wind tunnel

model span prevents disturbances from wall junctions to contribute the measurements along the centerline in the spanwise range of interest. The following flat plate coordinate system was used : the coordinate origin is located at the leading edge of flat plate, x (streamwise coordinate) is directed downstream and coincides with the flat plate centerline, z (spanwise coordinate) is directed along the leading edge, and y (wall-normal coordinate) is normal to the flat plate surface.

The experiments were performed at free stream velocity U_0=6.2 m/s. A Dantec Dynamics traversing three-coordinate system with automated, high resolution positioning with a mechanical solution adapted to CTA. The traversing mechanism was controlled by a sampling program written especially for these experiments in MATLAB. The traversing mechanism made it possible to perform spatial measurements with relative accuracy of 5.6 μm in all directions. Streamwise velocity inside the boundary layer was measured with constant 2 mm step in z-direction and 0.2 mm step in y-direction. Measurements were carried out in the central part of the plate in 80～100 mm range of the spanwise coordinate at several x stations. The spanwise range was chosen on a trial basis to cover the whole spanwise extent of the excited streak and small enough to minimize the consumption of time for the measurements. The range of measurements in x was restricted by capacity of traversing mechanism and test section design.

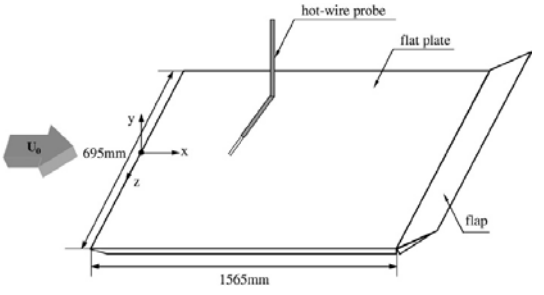

Fig. 2 Flat plate model and related coordinate system

Fig. 3 Flat plate model and hot wire installed in the test section

2.2 Microwing

The setup of the microwing (Fig. 4) with respect to the flat plate is shown schematically in Fig. 5. The axial vortex originated at the tip of a microwing with 0.6 mm thick and 5 mm wide symmetrical NACA 0012 profile manufactured of brass. Its edges and sides had 0.3 mm rounding-off radius. The wing was glued to a long cylindrical wooden support sting of 8 mm diameter. To minimize possible end effects and an influence

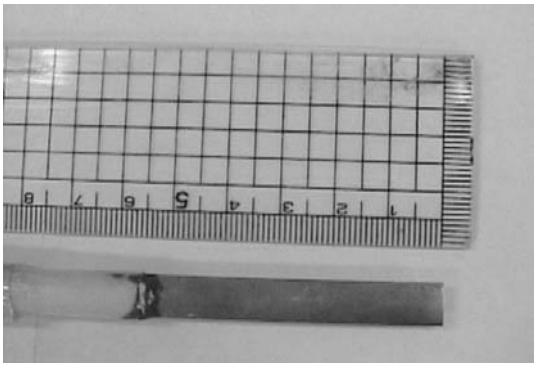

Fig. 4 Microwing

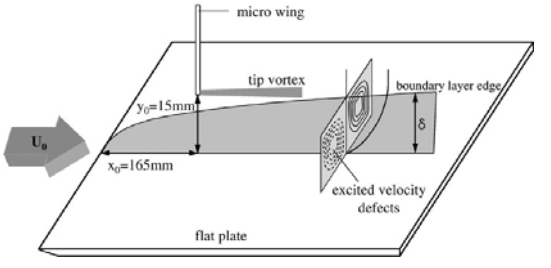

Fig. 5 The setup of microwing with respect to the flat plate

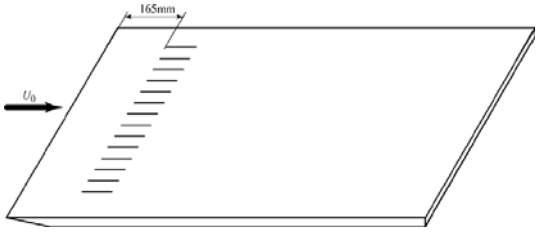

Fig. 6 Schematic diagram of surface roughness

of the sting, the microwing had 80 mm span. It was positioned at $x_0=165$ mm downstream from the leading edge above the flat plate at $y_0=15$ mm.

2.3 Roughness elements

In this study, the surface roughness was employed as an alternative way to excite the. This is a model of streak excitation by an array of obstacles. In this case the boundary layer is forced only locally in the vicinity of the roughness elements. A sketch of the experimental setup is given in Fig. 6. The row of 14 elements of $10\times2\times1.8$ mm^3 (LWH) was installed 165 mm downstream the leading edge. The application of the array of streak generators, rather than one as in the case of the microwing was stipulated by the wish to simplify spatial Fourier analysis of the disturbances and minimize side effects in the middle of the row. In contrast, the large width of the streak behind the microwing and difficulties of simultaneous adjustment of several microwings forced us to use only one tip vortex. Also, based on previous investigations in turbulent and transitional boundary layers, we expect that the riblets affect most efficiently, when the streak sizes are comparable with the riblet spacing.

2.4 Riblets

A removable riblet surface was mounted, as shown in Fig. 7. Triangular riblets with a square section were used. The leading edge of the riblets surface was 15 mm downstream of the microwing tip. The riblet surface was molded by vulcanite rubber. The leading edge was smoothed to remove the effect of the step. The riblets used in the present study were identical to those used in previous study of Boiko et al.(1997).

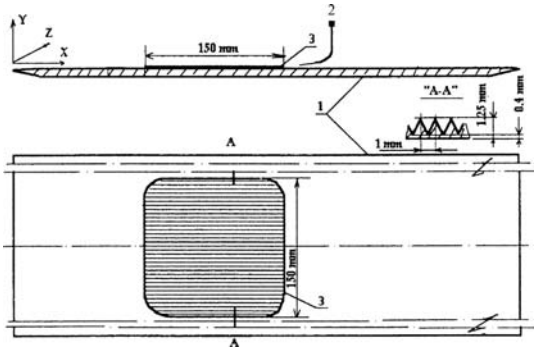

Fig. 7 A removable riblet surface mounted on the flat plate

3. Results and Discussion

3.1 Free stream turbulence measurement

Detailed studies of free stream turbulence level in the wind tunnel of Pusan National University were performed for the first time. The results are shown in Fig. 8. In present case the origin of y and z coordinates is located at the wall and that of x coordinate at the entrance to the test section. As seen, in the bulk of the flow the free-stream turbulence level $T_u=u'/U_0$ is below 0.15% and mean velocity distribution is smooth. Here u' is the r.m.s. streamwise disturbance velocity. The velocity becomes smaller and the disturbance level increases only close to the wall where thin turbulent boundary layer exists. In addition, it is found that the boundary layer becomes somewhat thicker downstream.

3.2 Microwing-induced streak measurement

The streamwise velocity defect caused by the tip vortex is shown in Fig. 9. As seen, the tip vortex exists in a wide downstream region behind the microwing. The absence of its significant spreading in spanwise direction and small decay rate indicate that the tip vortex is laminar. Riblet cover was located beginning from $x_0=180$ mm downstream the leading edge. It is 150 mm in both length and width with the edges being rounded. Leading edge of the cover smoothed to exclude appearance of step and separation. Previous results (Grek et al. 1995 ; Boiko et al. 1997) showed that this setup is suitable for testing the riblet effect

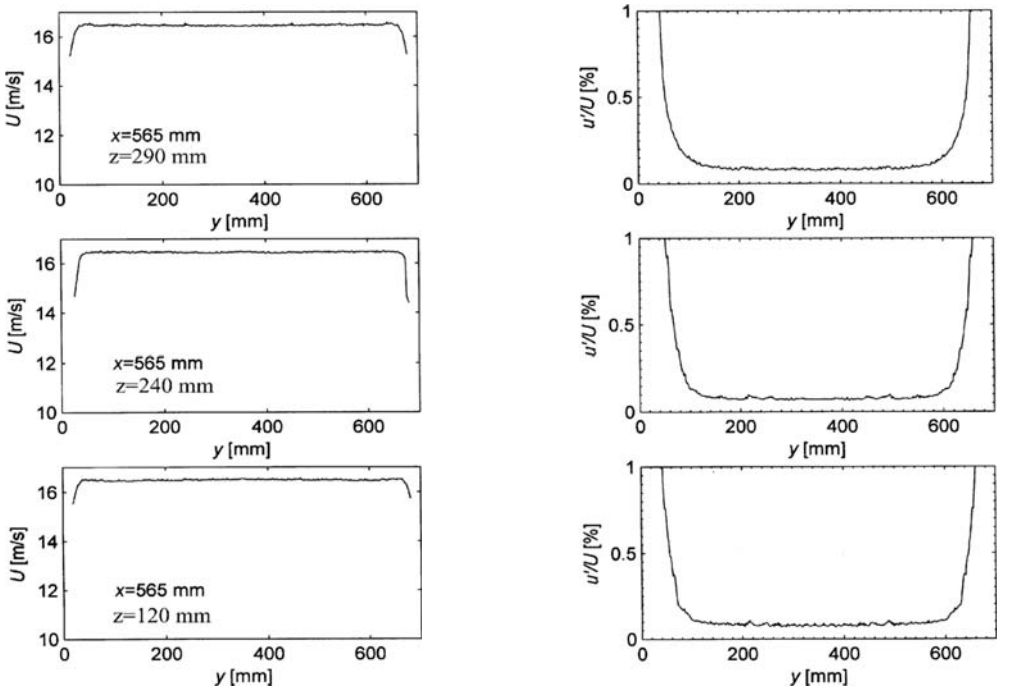

Fig. 8 Free stream mean velocity distribution in the wind tunnel test section (left) and corresponding disturbance level of streamwise velocity (right)

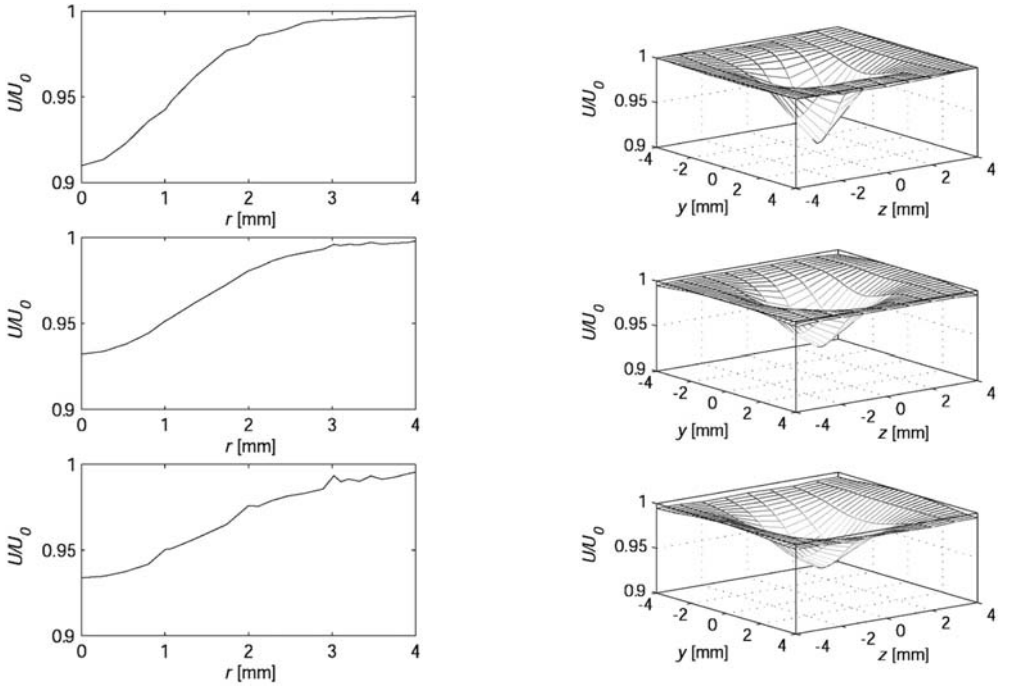

Fig. 9 Streamwise velocity defect in free stream due to the presence of the tip vortex behind the microwing. From top to down $\Delta x = x - x_0 = 45$, 102, 144 mm, Volume plot of the velocity defect (left) ; the velocity defect unwrapped using polar coordinates (right). The microwing tip located at $y_0 = 15$ mm

on structures specific for laminar-turbulent transition. In particular, by placing an auxiliary smooth plate with effective height equivalent to the riblet height, it has been shown that the leading edge of the riblet cover has no dominant effect on the observed phenomena. The excited streamwise velocity defects and excesses are shown in Fig. 10. The isolines at the bottom of the plots indicate that in both cases the intensity of the stationary streak is growing downstream, but velocity defects become somewhat smaller when the riblets are installed. In all the case the maximum of velocity distortions is located at $y/\delta^* \approx 1.2$, which is specific for the streaks in Blasius boundary layer. The value of the intensity reduction is demonstrated in more detail in Fig. 10.

The transition to turbulence is caused by travelling (unsteady) disturbances. Because of it, it is significant to look at their behavior (Fig. 11). As seen, the installation of riblets precludes the disturbance growth. The growth of unsteady disturbances inside a streak is usually associated with

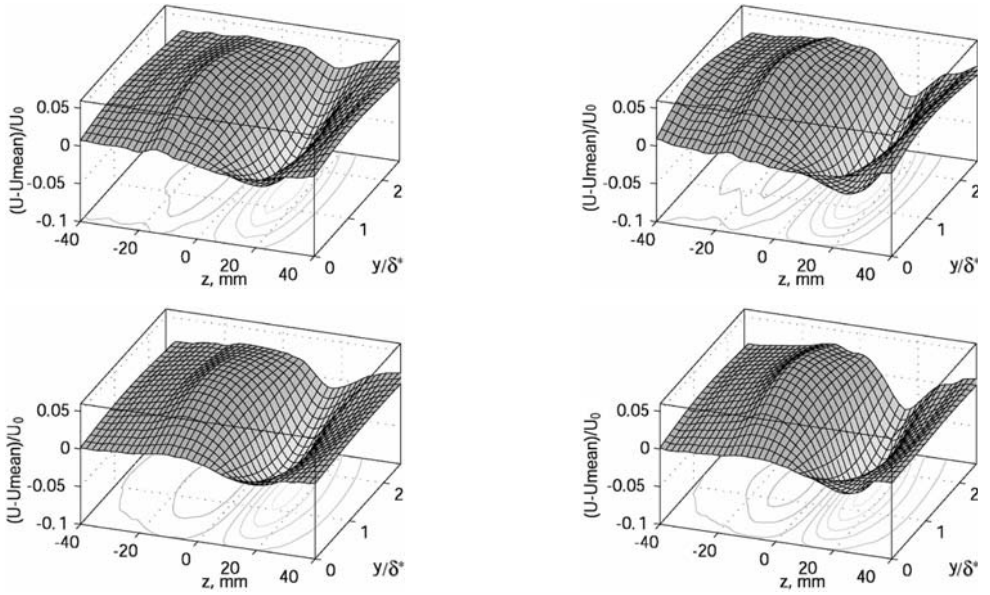

Fig. 10 Excited streamwise velocity defects and excesses without riblets (top) and with riblets (bottom) at $\Delta x = x - x_0 = 10$ (left) and 144 mm (right), Coordinate y is normalized to local displacement thickness δ^*, Contour plots are equidistant in all cases

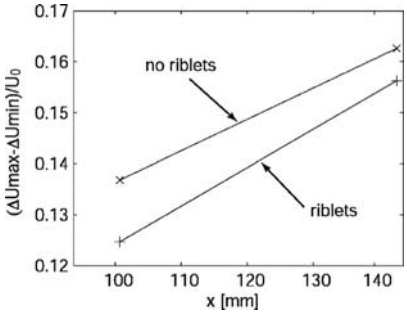

Fig. 11 Difference between the extremes of velocity defect and excess for the cases with and without riblets

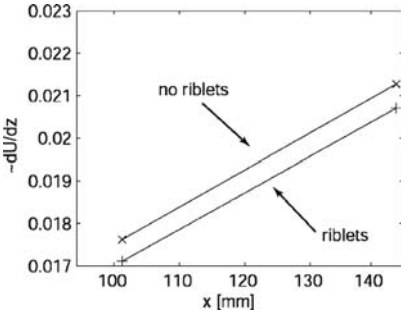

Fig. 12 Maximum values of spanwise velocity gradients with and without riblets

the so-called high-frequency secondary instability (loosely speaking, the streak development is considered as the primary 'instability'). From the classical Rayleigh theory of inviscid instability, local in space instability condition are expected when the mean velocity profile has inflection points (in other words, maximum gradient in wall-normal and spanwise directions). Such velocity profiles must be highly unstable to high-frequency disturbances. We approximated measured velocities by splines and used differentiation of spline functions to look at the values of the gradients (Fig. 12). Clearly, the presence of the riblets decreases the spanwise gradient and consequently weakens the instability condition. This can explain the decrease of disturbance intensity in Fig. 13.

3.3 Roughness-induced streak measurement

The experiments were performed at the same $U_0=6.2$ m/s and flat plate as above. In addition a dynamic loudspeaker was placed in the contraction chamber. The sound was used to excited

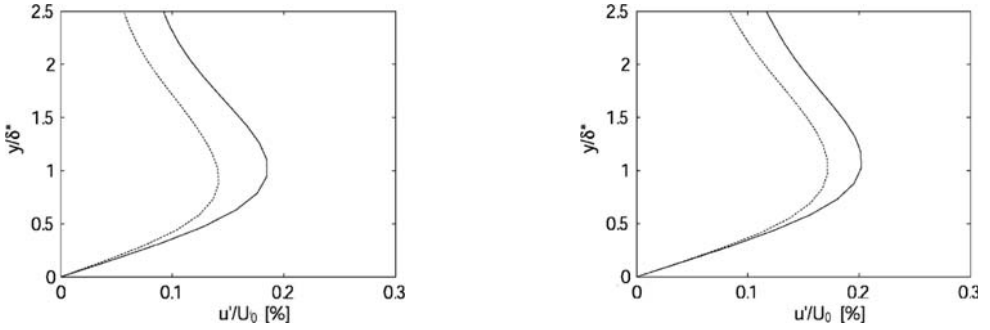

Fig. 13 R.m.s. values of streamwise velocity disturbances. $\Delta x=x-x_0=102$ (left) and 144 mm (right). Without riblets (solid lines), with riblets (dotted lines) Maximum values of spanwise velocity gradients with and without riblets

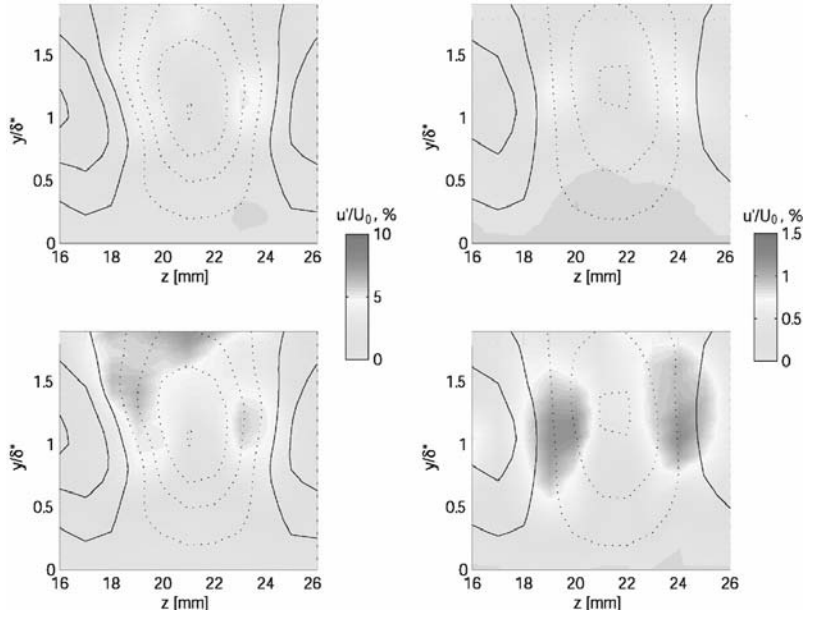

Fig. 14 Contour lines - equidistant velocity defect (dotted) and excess (solid). $\Delta x=262$ mm. Color contours -excited disturbances at $f=120$ Hz (top) and r.m.s. disturbances (bottom) without riblets (left) and with riblets (right)

controlled travelling disturbances in the generated streaks at $f=120$ Hz. The frequency was chosen on a trial basis to be from the range of the secondary instability. The sampling was synchronized with the sound excitation, so that phase information on the disturbance development can be extracted. Contour lines of the velocity defect and excess behind one of the roughness in the middle of the row are shown in Fig. 14. Two observations are remarkable : first, the riblets once again decrease the intensity of the streak (note the number of contours) and this decrease is much more pronounced than with the microwing setup ; second, both r.m.s. disturbances and those in a narrow band at $f=120$ Hz becomes much smaller (note different color levels on the left and right plots). Also, three regions of the disturbance localization are seen in Fig. 14. Figure 15 serves to

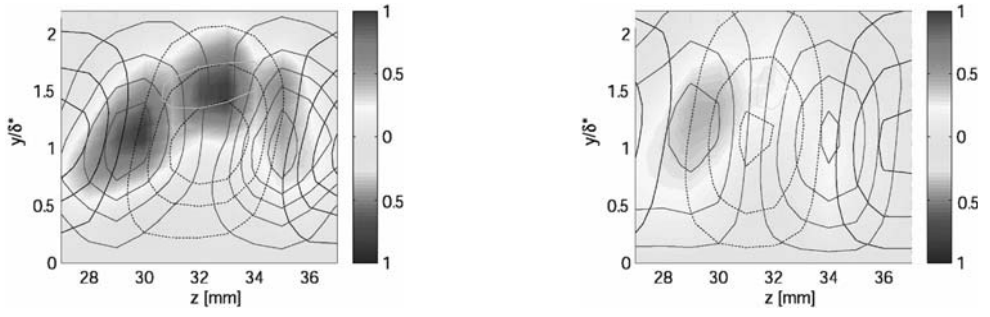

Fig. 15 Relation of the velocity gradients and disturbance maxima at $\Delta x=150$ mm. The spanwise velocity gradient and wall normal velocity gradient are shown by blue and green contour lines, respectively. Isolines of velocity defects and excess are shown by black dotted and solid lines, respectively. Color shows the location and intensity of disturbances at $f=120$ Hz

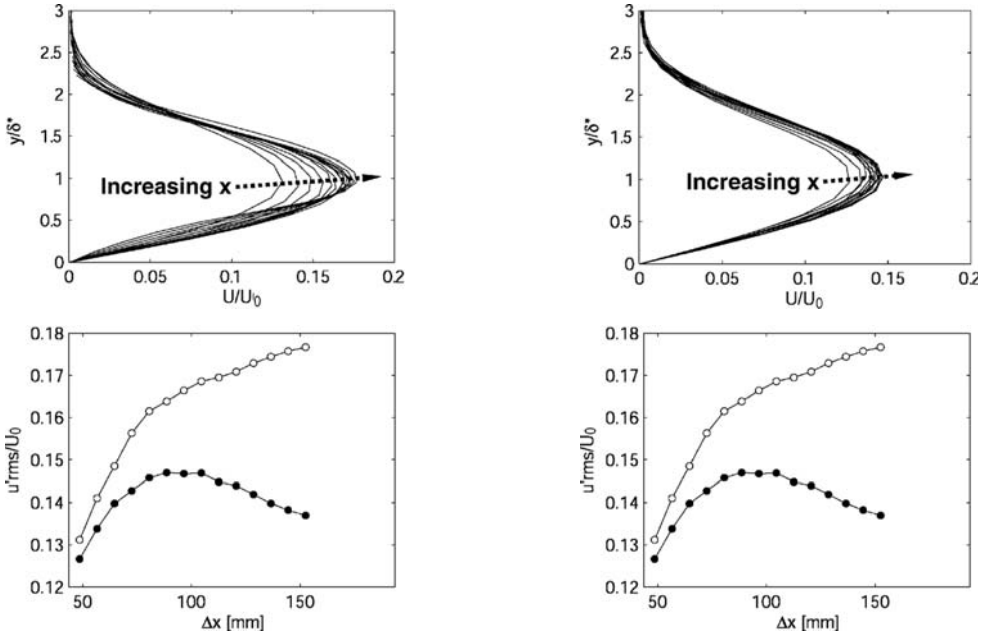

Fig. 16 Streak 'intensity' with (right) and without (left) riblets for $\Delta x=45\sim150$ mm at the top. Amplitude of r.m.s. disturbances (left) and those at $f=120$ Hz (right) at the bottom. Empty symbols – without riblets, filled symbols – with riblets

clarify their relation to the mean velocity gradients. The spanwise velocity gradients (calculated as before) and wall normal velocity gradient are shown by blue and green contour lines, respectively. Isolines of velocity defects and excess are shown by black dotted and solid lines, respectively. Color shows the location and intensity of disturbances with $f=120$ Hz. Clearly, the location of disturbance maximums almost perfectly coincides with the corresponding gradients. The growth of streak intensity and travelling disturbances is illustrated in Fig. 16. The streak profiles were obtained as standard deviations of the velocity difference from the mean value over one spanwise spacing between the roughness ($N=10$ is number of points measured in z-direction between neighboring roughness elements):

$$\Delta U(y)=\sum_{z=z_0}^{z=z_0+10\text{mm}}\sqrt{\frac{(U(y,z)-U_{mean}(y))^2}{N}}$$

$$U_{mean}(y)=\sum_{z=z_0}^{z=z_0+10\text{mm}}\frac{U(y,z)}{N}.$$

It is seen that the streak 'intensity' ΔU grows continuously downstream in both cases (Fig. 16, top), but the rate of growth and consequently the final amplitude of the streak (measured as the maximum value in the profiles) are smaller under the effect of the riblets. Corresponding behaviors of overall disturbances amplitudes and those at $f=120$ Hz are shown at the bottom of the figure. The growth of the disturbance amplitude at $f=120$ Hz measured in amplitude maximum is given in semi-logarithmic scale to emphasize that initial growth is virtually exponential, that is expected from the linear instability theory. Presence of the riblets leads to attenuation of the growth; therefore, the final amplitude of the wave at $f=120$ Hz becomes about 5 times smaller. As for the r.m.s. disturbances, they begin to decay from $\Delta x\approx 90$ mm indicating that the riblets significantly prolong the laminar regime.

4. Conclusions

Measurements on the effect of riblets on streaks excited by either tip vortex or roughness elements were carried out. Where intersect, the results are in accordance with previous findings. It was confirmed that that there is a certain rate between the riblets spacing and the characteristic spanwise size of the streaks, where the riblet effect is most pronounced. The riblets are shown to reduce the streak intensity and amplitude of travelling disturbances inside the streaks. It is speculated that the riblets act as a barrier to the cross-stream momentum, thereby reducing spanwise velocity nonuniformity which causes the streak instability and the travelling disturbances inside the streaks. The travelling disturbances consist of several modes with different phase velocities. The amplitude maxima of the modes are related to gradient maxima (inflection points) in streak streamwise velocity distributions. This indicates that the modes can be probably explained by the theory of secondary instability of streaks.

Acknowledgments

This work was financially supported by Pusan National University Grant, 2003 and by the ERC program (Advanced Ship Engineering Research Center) of MOST/KOSEF (grant No. R11-2002-104-05002-0).

References

Bechert, D. W. and Bartenwerfer, M., 1989, "The Viscous Flows on Surfaces with Longitudinal Ribs," *J. Fluid Mech.*, Vol. 206, pp. 105~129.

Blackwelder, R. F., 1983, "Analogies Between Transitional and Turbulent Boundary Layers," *Phys. Fluids*, Vol. 26, pp. 2807~2815.

Boiko, A. V., Klingmann, B. G., Kozlov, V. V. and Alfredsson, P. H., 1994, "Experiments in a Boundary Layer Subjected to Free Stream Turbulence. Part 2: The Role of TS-Waves in the Transition Process," *J. Fluid Mech.*, Vol. 281, pp. 219~245.

Boiko, A. V., Kozlov, V. V., Syzrantsev, V. V. and Scherbakov, V. A., 1997, "Transition control by Riblets in Swept Wing Boundary Layer with Embedded Streamwise Vortex," *European Jour-*

nal of Mechanics B/Fluids, Vol. 16, pp. 465~482.

Boiko, A. V., 2002, "Receptivity of a Flat Plate Boundary Layer to a Free Stream Axial Vortex," *European Journal of Mechanics B/Fluids*, Vol. 21, pp. 325~340.

Choi, H., Moin, P. and Kim, J., 1993, "Direct Numerical Simulation of Turbulent Flow Over Riblets," *J. Fluid Mech.*, Vol. 255, pp. 503~539.

Choi, H., Moin, P. and Kim, J., 1991, "On the Effect of Riblets in Fully Developed Laminar Channel Flow," *Phys. Fluids A*, Vol. 3, pp. 1892~1896.

Choi, K.-S., 1989, "Near-wall Structure of a Turbulent Boundary Layer with Riblets," *J. Fluid Mech.*, Vol. 208, pp. 417~458.

Coustols, E., 1992, "Performance of Internal Manipulators in Subsonic Three-Dimensional Flows," *Recent Developments in Turbulence* (*ed. Choi K.-S.*), Kluwer Academic Publishers, pp. 43~64.

Gad-el-Hak, M., 1990, "Control of Low-Speed Airfoil Aerodynamics," *AlAA J.*, Vol. 28, pp. 1537~1552.

Grek G. R., Kozlov, V. V. and Titarenko, S. V., 1993, "Investigation of Riblets Influence on Development of Vortex Generated by Suction/Blowing on a Flat Plate," *Soviet Journal of Applied Physics*, Vol. 6, pp. 31~45.

Grek, G. R., Kozlov, V. V., Titarenko, S. V. and Klingmann, B. G., 1995, "The Influence of Riblets on a Boundary Layer with Embedded Streamwise Vortices," *Phys. Fluids*, Vol. 7, pp. 2504~2506.

Kachanov, Y. S., 1994, "Physical Mechanisms of Laminar-Boundary-Layer Transition," *Ann. Rev. Fluid Mech.*, Vol. 26, pp. 411~482.

Klebanoff, P. D., Tidstrom, K. D. and Sargent, L. M., 1962, "The Three-Dimensional Nature of Boundary-Layer Instability," *J. Fluid Mech.*, Vol. 12, pp. 1~34

Kline, S. J., Reynolds, W. C., Schraub, F. A. and Runstadler, P. W., 1967, "The Structure of Turbulent Boundary Layer," *J. Fluid Mech.*, Vol. 30, pp. 741~773.

Luchini, P., Manzo, F. and Pozzi, A., 1991, "Resistance of a Grooved Surface to Parallel Flow and Cross-Flow," *J. Fluid Mech.*, Vol. 228, pp. 87~109.

Schneider, M. and Dinkelacker, A., 1992, "Drag Reduction by Means of Surface Riblets on an Inclined body of Revolution," *7th European Drag Reduction Working Meeting*, Submitted Abstract.

Walsh, M. J., 1983, "Riblets as a Viscous Drag Reduction Technique," *AIAA J.*, Vol. 21, pp. 485~486.

Westin, K. J. A., Boiko, A. V., Klingmann, B. G., Kozlov, V. V. and Alfredsson, P. H., 1994, "Experiments in a Boundary Layer Subjected to Free Stream Turbuelnce. Part 1 : Boundary Layer Structure and Receptivity," *J. Fluid Mech.*, Vol. 281, pp. 193~218.